Radiation Pressure of Radio Frequency Waves on Turbulence in Edge Plasmas

Abhay K. Ram[1, a)] and Kyriakos Hizanidis[2, b)]

[1)] *Plasma Science and Fusion Center, Massachusetts Institute of Technology, Cambridge, MA 02139. USA.*
[2)] *National Technical University of Athens, Zographou, Athens, Greece*

[a)] *Corresponding author: abhay@mit.edu*
[b)] *Electronic mail: kyriakos@central.ntua.gr*

Abstract. The scattering of radio frequency (RF) waves – lower hybrid and helicon waves – by a single cylindrical filament, embedded in a background plasma, is studied using a full-wave analytical theory. While a filament can affect the propagation of RF waves, the radiation force exerted by the waves can influence the filament. The force on a filament is determined using the Maxwell stress tensor. The radiation force can either pull the filament towards the RF source or push it away. The radiation force, in the two frequency ranges, is large enough to impact the motion of a filament and could be measured experimentally. Consequently, it may be possible to modify the edge turbulence using RF waves.

INTRODUCTION

The presence of blobs and filaments in the scrape-off layer of tokamak plasmas has been well documented experimentally (see, for example, [1]). Radio frequency (RF) electromagnetic waves, excited by antenna structures located near the wall of the fusion device, encounter these structures as the waves propagate towards the core plasma. Theoretical models, which are analytically tractable, have shown that blobs and filaments affect wave propagation and lead to reflection, refraction, diffraction, and shadowing [2, 3, 4]. A set of detailed computations have added more detail to the analytical results [5, 6]. While the filaments modify wave characteristics, the RF waves, in turn, can affect the blobs and filaments through radiation pressure. This paper is about the radiation force due to RF waves which is exerted on a cylindrical filament by lower hybrid waves and by helicon waves. The force is evaluated using the Maxwell stress tensor along with the Faraday-Ampere equation for the RF fields. In order to complete the analytical formulation, electromagnetic boundary conditions are imposed on the surface of the filament. For representative plasma parameters, the force due to lower hybrid waves and helicon waves on a cylindrical filament is computed numerically. The radiation force can either pull the filament towards the RF source or push it away. The direction of the force depends on the wave frequency and on the relative densities between the background plasma and the plasma inside the filament.

SCATTERING OF WAVES BY A CYLINDRICAL FILAMENT

We assume a uniform cylindrical plasma filament of radius a, embedded in a uniform background plasma, with its axis aligned along the magnetic field line (Fig. 1a). While the density inside and outside the filament can be different, the magnetic field is constant everywhere and the plasma is cold – the plasma permittivity does not include any thermal effects. An incoming plane wave propagates in the background plasma before encountering the filament. From the Faraday and Ampere equations, the spatial evolution of the electric field of a RF wave is,

$$\nabla \times \left(\nabla \times \vec{E}\,(\vec{r}) \right) - \frac{\omega^2}{c^2} \overleftrightarrow{\mathbf{K}}(\vec{r}) \,.\, \vec{E}\,(\vec{r}) \;=\; 0, \tag{1}$$

where the time dependence of all fields is of the form $\exp(-i\omega t)$. The propagation vector of the incident RF wave is in the x-y plane and of the form $\vec{k} = k_\perp \hat{x} + k_\parallel \hat{z}$ with $\hat{x}$ and $\hat{z}$ being the unit vectors along the x and z directions, respectively. For a homogeneous medium, a simple rotation about the z-axis will ensure this particular form of $\vec{k}$. In this coordinate system, the magnetic field is $\vec{B}_0 = B_0 \hat{z}$. The cold plasma permittivity tensor $\overleftrightarrow{\mathbf{K}}$ is,

$$\overleftrightarrow{\mathbf{K}} \;=\; \begin{pmatrix} K_{xx} & -iK_{xy} & 0 \\ iK_{xy} & K_{xx} & 0 \\ 0 & 0 & K_{zz} \end{pmatrix}, \tag{2}$$

where,

$$K_{xx} = 1 - \frac{\omega_{pe}^2}{\omega^2 - \omega_{ce}^2} - \sum_i \frac{\omega_{pi}^2}{\omega^2 - \omega_{ci}^2},$$
$$K_{xy} = -\frac{\omega_{ce}}{\omega} \frac{\omega_{pe}^2}{\omega^2 - \omega_{ce}^2} + \sum_i \frac{\omega_{ci}}{\omega} \frac{\omega_{pi}^2}{\omega^2 - \omega_{ci}^2}, \tag{3}$$
$$K_{zz} = 1 - \frac{\omega_{pe}^2}{\omega^2} - \sum_i \frac{\omega_{pi}^2}{\omega^2},$$

ω_{pe} (ω_{pi}) and ω_{ce} (ω_{ci}) are the electron (ion) angular plasma and angular cyclotron frequencies, respectively, and the summation is over all the ion species in the plasma.

The dispersion tensor for the plasma waves is,

$$\overleftrightarrow{\mathbf{D}} = \frac{c^2}{\omega^2} \left(\vec{k}\vec{k} - k^2 \overleftrightarrow{\mathbf{I}} \right) + \overleftrightarrow{\mathbf{K}}, \tag{4}$$

where $\overleftrightarrow{\mathbf{I}}$ is the identity tensor and $\vec{k}\vec{k}$ is a dyadic. The dispersion relation for the waves is $\mathscr{D}\left(\vec{k}, \omega\right) \equiv \det\left(\overleftrightarrow{\mathbf{D}}\right) = 0$, where det denotes the determinant of the second rank tensor. Assuming that $k_\parallel$, ω, ω_{pe}, ω_{pi}, ω_{ce}, and ω_{ci} are all prescribed, the dispersion relation $\mathscr{D}\left(k_\perp, k_\parallel, \omega\right) = 0$ is biquadratic in $k_\perp$.

The wave fields inside the filament and the wave fields of the scattered waves in the background plasma can be obtained from (1). The Faraday-Ampere equation is solved in cylindrical coordinates subject to the boundary conditions [3],

$$\hat{\rho} \times \left(\vec{E}_I + \vec{E}_S \right) \Big|_{\rho=a} = \hat{\rho} \times \vec{E}_F \Big|_{\rho=a}, \tag{5}$$
$$\hat{\rho} \times \left(\vec{B}_I + \vec{B}_S \right) \Big|_{\rho=a} = \hat{\rho} \times \vec{B}_F \Big|_{\rho=a}, \tag{6}$$

where $\hat{\rho}$ is the outward pointing normal unit vector at the interface of the filament, ρ is the radial coordinate, and all fields are evaluated at the surface of the filament $\rho = a$. The subscripts I, S, and F denote the incoming RF field, the scattered field (outside the filament), and the field inside the filament, respectively.

MAXWELL STRESS TENSOR – RADIATION FORCE ON A FILAMENT

The electromagnetic fields obtained from the scattering equation (1), along with the dispersion tensor (4) and the boundary conditions (5)-(6), can be used to evaluate the Maxwell stress tensor [7, 8]. For complex electromagnetic wave fields, the stress tensor is,

$$\overleftrightarrow{\mathbf{T}} = \vec{E}_R \vec{D}_R + \vec{H}_R \vec{B}_R - \frac{1}{2} \left(\vec{E}_R \cdot \vec{D}_R + \vec{H}_R \cdot \vec{B}_R \right) \overleftrightarrow{\mathbf{I}}, \tag{7}$$

where the subscript R indicates the real part of the associated field; the first two terms on the right hand side are dyadics, $\overleftrightarrow{\mathbf{I}}$ is the identity tensor, $\vec{H}$ is the magnetic intensity, and $\vec{B} = \mu_0 \vec{H}$. Using the relationship between $\vec{D}$ and $\vec{E}$, the time average over one period of the wave cycle yields,

$$\left\langle \overleftrightarrow{\mathbf{T}} \right\rangle = \frac{1}{2} \mathrm{Re} \left[\varepsilon_0 \vec{E}\, \overleftrightarrow{\mathbf{K}}^* \cdot \vec{E}^* + \mu_0 \vec{H} \vec{H}^* - \frac{1}{2} \left(\varepsilon_0 \vec{E} \cdot \overleftrightarrow{\mathbf{K}}^* \cdot \vec{E}^* + \mu_0 \left| \vec{H} \right|^2 \right) \overleftrightarrow{\mathbf{I}} \right], \tag{8}$$

where Re indicates the real part and * the complex conjugate.

In the cylindrical coordinate system, the time-averaged force on a filament of axial length L is [7, 9, 10],

$$\overrightarrow{\mathscr{F}} = \int \left\langle \overleftrightarrow{\mathbf{T}} \right\rangle \cdot d\boldsymbol{A} = a \int_0^L \int_0^{2\pi} \left\langle \overleftrightarrow{\mathbf{T}}(\rho = a) \right\rangle \cdot \hat{\rho}, \tag{9}$$

where the elemental area on the surface of the filament is $d\boldsymbol{A} = a\,d\phi\,dz\;\hat{\rho}$, with ϕ being the azimuthal coordinate around the axis of the filament. On the surface of the filament,

$$\left\langle \overleftrightarrow{\mathbf{T}}(\rho = a) \right\rangle \cdot \hat{\rho} \;=\; \left\langle \overleftrightarrow{\mathbf{T}}(\rho = a) \right\rangle_b \cdot \hat{\rho} - \left\langle \overleftrightarrow{\mathbf{T}}(\rho = a) \right\rangle_f \cdot \hat{\rho}, \tag{10}$$

where the subscript b indicates that the tensor is evaluated for fields in the background plasma – the incident and the scattered fields, and the subscript f is for fields inside the filament. The negative sign on the right hand side is due to the inward pointing normal for the filamentary fields. Equation (10) is a vector equation whose cylindrical components are determined using the boundary conditions (5) and (6). After some algebra we find that,

$$\begin{aligned} \hat{\rho} \cdot \left\langle \overleftrightarrow{\mathbf{T}}(\rho = a) \right\rangle \cdot \hat{\rho} \;=\; & \frac{\varepsilon}{4} \Big[K_{xx}^B \left| E_{I\rho} + E_{S\rho} \right|^2 - K_{xx}^F \left| E_{F\rho} \right|^2 + \\ & \left(K_{xx}^F - K_{xx}^B \right) \left| E_{F\phi} \right|^2 + \left(K_{zz}^F - K_{zz}^B \right) \left| E_{Fz} \right|^2 \Big]_{\rho = a}, \end{aligned} \tag{11}$$

$$\hat{\phi} \cdot \left\langle \overleftrightarrow{\mathbf{T}}(\rho = a) \right\rangle \cdot \hat{\rho} \;= 0, \tag{12}$$

$$\hat{z} \cdot \left\langle \overleftrightarrow{\mathbf{T}}(\rho = a) \right\rangle \cdot \hat{\rho} \;= 0. \tag{13}$$

The superscripts B and F indicate that these elements of the permittivity tensor are evaluated for plasma parameters corresponding to the background and filamentary plasmas, respectively. The subscripts in the electric fields include the components corresponding to the cylindrical coordinate system. The right hand side is evaluated at the surface of the filament. From equations (12)-(13) we note that the RF fields do not induce any shear forces on the filament; the only force is in the radial direction. The radial component (11) is a function of the azimuthal angle ϕ and is independent of z; the z variation of the fields is $\exp(ik_z z)$ and is accounted for in the matching of wave phases at the surface of the filament. The radial force can lead to two possible effects – spatial displacement of the filament and its azimuthal distortion.

The only component of $\overrightarrow{\mathscr{F}}$ in (9) is in the $\hat{\rho}$ direction. Since (11) has no variation along z, the radial force per unit axial length has two Cartesian components in the x and y directions,

$$\begin{pmatrix} \mathscr{F}_x \\ \mathscr{F}_y \end{pmatrix} \;=\; a \int_0^{2\pi} d\phi \begin{pmatrix} \cos\phi \\ \sin\phi \end{pmatrix} \hat{\rho} \cdot \left\langle \overleftrightarrow{\mathbf{T}}(\rho = a) \right\rangle \cdot \hat{\rho}. \tag{14}$$

We have redefined the force vector in (9) as force per unit axial length.

The power flux of the incident wave is

$$S_I \;=\; \left| \left\langle \vec{S}_I \right\rangle \right| \;=\; \frac{1}{2} \sqrt{\frac{\varepsilon_0}{\mu_0}}\, |\mathscr{E}_0|^2 \tag{15}$$

where $\left\langle \vec{S}_I \right\rangle$ is the time-averaged Poynting vector and $\mathscr{E}_0$ is the electric field amplitude of the incident wave. The force on a filament per unit incident power flux is,

$$\begin{pmatrix} \widetilde{\mathscr{F}}_x \\ \widetilde{\mathscr{F}}_y \end{pmatrix} \;=\; \frac{1}{S_I} \begin{pmatrix} \mathscr{F}_x \\ \mathscr{F}_y \end{pmatrix} \quad \frac{\mathrm{N\ m^{-1}}}{\mathrm{W\ m^{-2}}}. \tag{16}$$

The units expressed on the right hand side are Newton per meter (of axial length) for the force and Watt per square meter for the power flux. The stress force on the filament induces an acceleration,

$$\begin{pmatrix} \mathfrak{a}_x \\ \mathfrak{a}_y \end{pmatrix} \;=\; \frac{1}{\mathfrak{m}} \begin{pmatrix} \widetilde{\mathscr{F}}_x \\ \widetilde{\mathscr{F}}_y \end{pmatrix}, \tag{17}$$

where $\mathfrak{m}$ is the mass of a cylindrical filament of length 1 m and radius a m.

RADIATION FORCE AND INDUCED ACCELERATION – NUMERICAL RESULTS

In this section we give numerical results for the radiation force on a filament of axial length 1 m. The plasma inside and outside the filament is composed of deuterons. Then the mass of the filament is $\mathfrak{m} = 1.05 \times 10^{-26}\, a^2\, n_{ef}$ kg, where n_{ef} is the electron density inside the filament. The acceleration induced by the force is evaluated for an input wave power of 1 kW/m^2. From all numerical simulations that have been carried out for different density regimes and, notably, for different RF waves, we find $\widetilde{\mathscr{F}_y} = 0$, implying $\mathfrak{a}_y = 0$ [10]. Thus, we will provide results for $\widetilde{\mathscr{F}_x}$ and $\mathfrak{a}_x$. We consider RF waves in two different frequency regimes – the lower hybrid waves and the helicon waves. The incoming wave is propagating along the $+\hat{x}$ direction. Consequently, a positive force is pushing the filament away from the source of the incoming wave while a negative force is pulling in the filament.

Lower Hybrid Waves

Consider lower hybrid waves with frequency $\nu = \omega/2\pi = 4.6$ GHz and a parallel index of refraction $n_\parallel = ck_\parallel/\omega = 2$ propagating in a plasma with $B_0 = 4.5$ T. Let the electron density of the background plasma be $n_{eb} = 2.25 \times 10^{19}$ m^{-3}, and inside the filament $n_{ef} = 2.5 \times 10^{19}$ m^{-3}; thus, $n_{ef} > n_{eb}$. The radiation force on the filament due to the slow and fast waves, respectively, is,

$$\widetilde{\mathscr{F}_x}\Big|_S \;=\; -4.26\;\frac{\text{nN m}^{-1}}{\text{kW m}^{-2}}, \qquad \widetilde{\mathscr{F}_x}\Big|_F \;=\; 87.71\;\frac{\text{nN m}^{-1}}{\text{kW m}^{-2}}. \tag{18}$$

It is interesting to note that the slow wave tends to pull the higher density filament towards the source of lower hybrid waves, while the fast wave pushes it away. The fast wave exerts radiation pressure which, in magnitude, is much larger than due to the slow wave. The induced acceleration by the slow and fast waves, respectively, is,

$$\mathfrak{a}_x\Big|_S \;=\; -1.62 \times 10^2\;\text{m sec}^{-2}, \qquad \mathfrak{a}_x\Big|_F \;=\; 3.34 \times 10^3\;\text{m sec}^{-2}. \tag{19}$$

If we choose the density inside the filament to be $n_{ef} = 2.0 \times 10^{19}$ m^{-3} while keeping the background density n_{eb} same as above, then $n_{ef} < n_{eb}$ and the radiation force due to slow and fast waves, respectively, is,

$$\widetilde{\mathscr{F}_x}\Big|_S \;=\; 4.23\;\frac{\text{nN m}^{-1}}{\text{kW m}^{-2}}, \qquad \widetilde{\mathscr{F}_x}\Big|_F \;=\; -56.13\;\frac{\text{nN m}^{-1}}{\text{kW m}^{-2}}. \tag{20}$$

The slow wave pushes the lower density filament away from the source while the fast wave pulls the filament in towards the source. Upon comparing with (18), we note that there is a reversal in the sign of the force due to slow and fast waves. Furthermore, the magnitude of the force changes considerably for the fast wave while remaining essentially the same for the slow wave. This is due to the internal wave structures inside the filament [10]. From the results in (18) and (20), we notice that the slow wave will tend to increase the density in front of the wave guides launching the lower hybrid waves, while the fast wave will tend to decrease the density as it pushes away the higher density filaments. The induced acceleration due to the forces in (20) is, respectively,

$$\mathfrak{a}_x\Big|_S \;=\; 2.01 \times 10^2\;\text{m sec}^{-2}, \qquad \mathfrak{a}_x\Big|_F \;=\; -2.67 \times 10^3\;\text{m sec}^{-2}. \tag{21}$$

Fast Helicon Waves

For the parameters of interest: $\nu = 476$ MHz, $B_0 = 1.4$ T, and $n_\parallel = 4$, the dispersion relation for the fast helicon wave as a function of electron density is shown in Fig. 1b. The fast wave does not propagate for densities less than the cutoff density $n_{ec} \approx 3.5 \times 10^{18}$ m^{-3}. In the density range shown, the slow helicon wave propagates for densities less than the density corresponding to the lower hybrid resonance (dotted vertical line in Fig. 1b) $n_{elhr} \approx 2.25 \times 10^{19}$ m^{-3}. Even though we are calculating the radiation pressure due to the fast helicon wave, the filament can induce coupling of some incoming power to the slow helicon wave. The slow wave will be part of the scattered fields and fields inside the filament. The calculations for the radiation pressure are divided into three distinct regions in electron density space. For low densities, the fast helicon wave is an evanescent mode while the slow helicon wave is a propagating mode. For medium densities, both slow and fast waves are propagating modes, while for high densities only the fast helicon wave is a propagating mode.

Low Density Region $n_e < n_{ec}$

For a filament with density $n_{ef} = 3.75 \times 10^{17}$ m^{-3} embedded in a background plasma with density $n_{eb} = 5 \times 10^{17}$ m^{-3}, so that $n_{ef} < n_{eb}$, the radiation force and the induced acceleration of the filament are, respectively,

$$\widetilde{\mathscr{F}_x}\Big|_F = -61.2 \ \frac{\text{nN m}^{-1}}{\text{kW m}^{-2}} \qquad \mathfrak{a}_x\Big|_F = -1.6 \times 10^5 \ \text{m sec}^{-2}. \tag{22}$$

If, instead, we choose $n_{ef} = 7 \times 10^{17}$ m^{-3} leaving n_{eb} unchanged, then $n_{ef} > n_{eb}$ and the radiation force and the induced acceleration are, respectively,

$$\widetilde{\mathscr{F}_x}\Big|_F = 63.3 \ \frac{\text{nN m}^{-1}}{\text{kW m}^{-2}} \qquad \mathfrak{a}_x\Big|_F = 8.6 \times 10^4 \ \text{m sec}^{-2}. \tag{23}$$

From (22) and (23), we note that, in the low density regime, the fast helicon waves pull in lower density (compared to background density) filaments and push out higher density filaments away from the RF source. Thus, the density in front of the antenna will tend to decrease.

Medium Density Region $n_{ec} < n_e < n_{elhr}$

In the medium density region the slow and fast helicon waves are propagating modes. For $n_{ef} = 6 \times 10^{18}$ m^{-3} and $n_{eb} = 9 \times 10^{18}$ m^{-3}, $n_{ef} < n_{eb}$ and the radiation force and the induced acceleration are, respectively,

$$\widetilde{\mathscr{F}_x}\Big|_F = -6.5 \times 10^3 \ \frac{\text{nN m}^{-1}}{\text{kW m}^{-2}} \qquad \mathfrak{a}_x\Big|_F = -10^6 \ \text{m sec}^{-2}. \tag{24}$$

If, instead, $n_{ef} = 1.2 \times 10^{19}$ m^{-3} while n_{eb} remains the same, $n_{ef} > n_{eb}$ and the radiation force and the induced acceleration are, respectively,

$$\widetilde{\mathscr{F}_x}\Big|_F = -5 \times 10^4 \ \frac{\text{nN m}^{-1}}{\text{kW m}^{-2}} \qquad \mathfrak{a}_x\Big|_F = -3.9 \times 10^6 \ \text{m sec}^{-2}. \tag{25}$$

From (24) and (25), we find that, in the medium density regime, the fast helicon waves pull in lower and higher density filaments towards the RF source, leading to an increase in density in front of the antenna. These results are quite different from those for the low density regime where there is a change in direction of the radiation force as the density inside the filament increases from less than the background density to greater than the background density. Also, upon comparing with (22) and (23), we find that the radiation force on a filament due to a propagating fast helicon wave is much larger than due to an evanescent wave.

High Density Region $n_e > n_{elhr}$

In this region the fast helicon wave is a propagating wave while the slow helicon wave is an evanescent mode. For $n_{ef} = 2.4 \times 10^{19}$ m^{-3} and $n_{eb} = 3 \times 10^{19}$ m^{-3}, $n_{ef} < n_{eb}$ and the radiation force and the induced acceleration are, respectively,

$$\widetilde{\mathscr{F}_x}\Big|_F = -2.5 \times 10^4 \ \frac{\text{nN m}^{-1}}{\text{kW m}^{-2}} \qquad \mathfrak{a}_x\Big|_F = -9.9 \times 10^5 \ \text{m sec}^{-2}. \tag{26}$$

If the density inside the filament is increased to $n_{ef} = 3.6 \times 10^{19}$ m^{-3} while keeping n_{eb} fixed, $n_{ef} > n_{eb}$ and the radiation force and the induced acceleration are, respectively,

$$\widetilde{\mathscr{F}_x}\Big|_F = -8.8 \times 10^3 \ \frac{\text{nN m}^{-1}}{\text{kW m}^{-2}} \qquad \mathfrak{a}_x\Big|_F = -2.3 \times 10^5 \ \text{m sec}^{-2}. \tag{27}$$

As in the medium density region, the results in (26) and (27) indicate that the fast helicon waves pull in lower and higher density filaments towards the RF source, leading to an increase in density in front of an antenna.

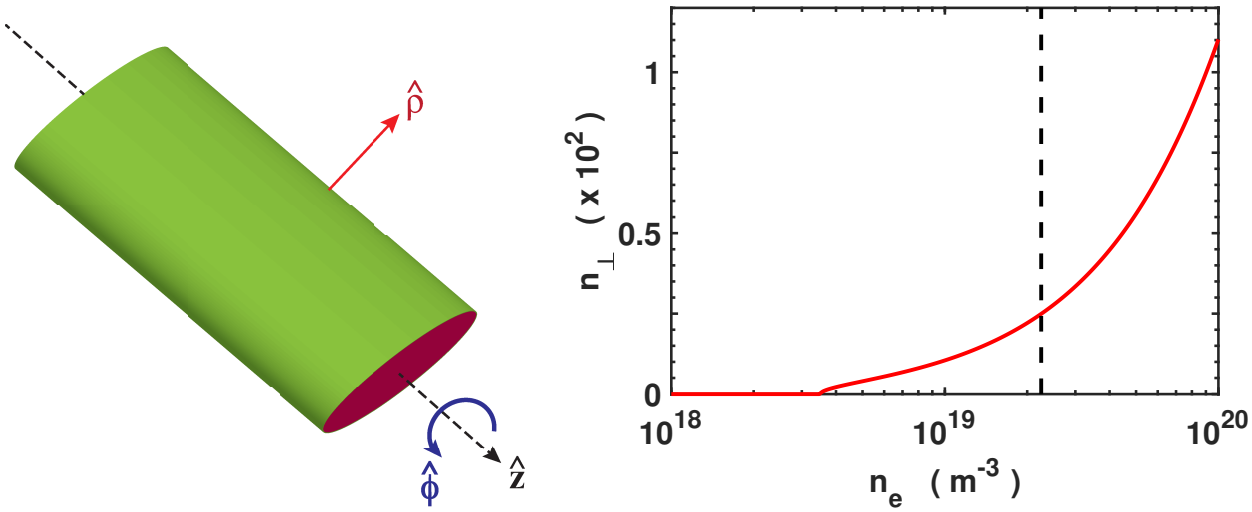

(a) (b)

FIGURE 1: (a) The coordinate system with respect to the cylindrical filament: $\hat{\rho}$ is outward pointing normal to the surface, $\hat{\phi}$ is the unit vector in the azimuthal direction, and the ambient magnetic field is $\vec{B}_0 = B_0\hat{z}$. (b) The dispersion relation for a fast helicon wave (solid line): $n_\perp = ck_\perp/\omega$ as a function of electron density n_e in a plasma composed of electrons and deuterons. The relevant parameters are $B_0 = 1.4$ T, $\nu = 476$ MHz, and $n_\parallel = 4$. The dashed line is the location of the lower hybrid resonance – the slow helicon wave propagates for densities less than this density. The fast helicon wave is cutoff for $n_e < n_{ec} \approx 3.5 \times 10^{18}$ m^{-3}.

CONCLUSION

The RF induced radiation force on cylindrical filaments can either pull the filament in towards the RF source or push it away. The force is large enough that its effect on filaments could be observed in experiments. Regardless of the direction of the radiation force, the RF waves can modify the density profile in front of the launching antenna. Two different RF waves do not induce similar trends in the radiation force. A comparison of the forces induced by lower hybrid waves and by fast helicon waves illustrate this point.

ACKNOWLEDGMENTS

AKR was supported by the US Department of Energy Grant numbers DE-FG02-91ER-54109 and DE-FC02-01ER54648.

REFERENCES

1. O. Grulke, J. L. Terry, I. Cziegler, B. Labombard and O. E. Garcia, Nucl. Fusion **54**, 043012-1-043012-12 (2014).
2. A. K. Ram, K. Hizanidis, and Y. Kominis, Phys. Plasmas **20**, 056110-1-056110-10 (2013).
3. A. K. Ram and K. Hizanidis, Phys. Plasmas **23**, 022504-1-022504-17 (2016).
4. J. R. Myra and D. A. D'Ippolito, Phys. Plasmas **17**, 102510 (2010).
5. A. Köhn, E. Holzhauer, J. Leddy, M. B. Thomas, and R. G. L. Vann, Plasma Phys. Controlled Fusion **58**, 105008-1–105008-9 (2016).
6. Z. C. Ioannidis, A. K. Ram, K. Hizanidis, and I. G. Tigelis, Phys. Plasmas **24**, 102115-1–102115-13 (2017).
7. A. Bers, *Plasma Physics and Fusion Plasma Electrodynamics, Volume 2* (Oxford University Press, New York, 2016).
8. W. K. H. Panofsky and M. Phillips, *Classical Electricity and Magnetism* (Dover Publications, New York, 2005).
9. J. A. Stratton, *Electromagnetic Theory* (McGraw-Hill, New York, 1941).
10. S. I. Valvis, A. K. Ram, and K. Hizanidis, J. Plasma Phys. **87**, 905870612-1-905870612-37 (2021).